AIAA JOURNAL
Vol. 45, No. 4, April 2007

Design and Wind-Tunnel Verification of Low-Noise Airfoils for Wind Turbines

T. Lutz,* A. Herrig,† W. Würz,‡ M. Kamruzzaman,† and E. Krämer§
Universität Stuttgart, 70550 Stuttgart, Germany

DOI: 10.2514/1.27658

In this paper a method for the prediction of the airfoil trailing-edge far-field noise is presented. The model employs the airfoil analysis code XFOIL to determine the initial and boundary conditions for a subsequent boundary-layer analysis using the finite-difference code EDDYBL featuring a Reynolds stress turbulence model that finally provides the input data for the noise prediction by a modified TNO Institute of Applied Physics model. The prediction scheme was applied in the European silent rotors by acoustic optimization project to design new, quieter airfoils for the outer blade region of three different wind turbines in the megawatt class. The objective was to reduce the airfoil self-noise without loss in aerodynamic performance. Wind-tunnel tests showed that a noticeable noise reduction could be achieved compared with the airfoils currently in use. Moreover, the aerodynamic performance could be improved in the design region as well.

Nomenclature

C	=	empirical constant, Kolmogorov spectrum
c	=	chord length
c_L	=	lift coefficient
c_0	=	speed of sound
$E(k)$	=	kinetic energy density spectrum
f	=	frequency
k, $\boldsymbol{k}$	=	wave number, wave number vector
k_e	=	wave number of the energy-bearing eddies
k_T	=	turbulence kinetic energy
L	=	wetted length of the trailing edge
L_p	=	total sound pressure level
L/D	=	lift-to-drag ratio
p	=	fluctuating pressure
$\hat{p}$	=	Fourier transform of p
P	=	wave number frequency spectrum
R	=	distance to the observer from source point
R_{ij}	=	velocity spatial correlation tensor
Re	=	Reynolds number
S	=	far-field pressure density
t	=	time
U_i, u_i	=	freestream, fluctuation velocity components
U_∞, U_c	=	reference and convective velocity
y_i, x, y, z	=	Cartesian coordinates
Γ	=	Euler gamma function
δ	=	boundary-layer thickness
ε	=	turbulent dissipation rate
Λ_2	=	vertical integral length scale
λ	=	wavelength
ρ_0	=	density
Φ_{ij}	=	spectrum of velocity fluctuation
Φ_m	=	moving axis spectrum
ω	=	angular frequency

Subscripts

cen	=	center
trans	=	transition location

Presented as Paper 3322 at the 24th AIAA Applied Aerodynamics Conference, San Francisco, CA, 5–8 June 2006; received 8 September 2006; revision received 1 January 2007; accepted for publication 2 January 2007.

*Senior Researcher, Institute of Aerodynamics and Gas Dynamics, Pfaffenwaldring 21. AIAA member.
†Research Engineer, Institute of Aerodynamics and Gas Dynamics, Pfaffenwaldring 21. AIAA member.
‡Senior Researcher, Institute of Aerodynamics and Gas Dynamics, Pfaffenwaldring 21.
§Professor, Head of the Institute, Institute of Aerodynamics and Gas Dynamics, Pfaffenwaldring 21.

I. Introduction

NOISE emission is one of the major obstacles for a further spread of onshore wind turbines and significantly limits public acceptance. Tightened noise regulations force the wind turbine manufacturers to make serious efforts in noise reduction. Although mechanical noise can efficiently be reduced by well-established engineering approaches, the flow-induced noise emitted from the blades is more complex to comprehend and eliminate and, therefore, represents the current focus for further noise reduction. Different flow-induced noise sources can be distinguished, e.g., tip noise, inflow-turbulence noise, blunt trailing-edge noise, or turbulent boundary-layer trailing-edge interaction noise. Previous investigations including field tests [1] showed that the trailing-edge noise remains the most dominant noise source of modern wind turbines. This particular noise basically stems from an interaction of the turbulent eddies within the boundary layer and the associated pressure fluctuations with the trailing edge of the rotor blades.

Because the state of the turbulence in the vicinity of the trailing edge is determined by the development of the boundary layer and thus by the shape of the pressure distribution along the blade section, it is obvious that the noise emission can be influenced and finally reduced by an adequate design of the airfoil. Numerical aeroacoustic simulations based on computational fluid dynamics (CFD) flowfield analyses are computationally very intensive and the application is restricted to acoustic analyses or low-degree-of-freedom airfoil optimization. Marsden et al. [2] considered five design variables in their acoustic optimization of an airfoil trailing-edge shape which required less than 20 evaluations. They performed costly large-eddy simulations as a basis for the acoustic computations that rely on the Ffowcs–Williams and Hall (FW-H) integral solution of the Lighthill equation [3]. Greschner et al. [4] applied unsteady Reynolds-averaged Navier–Stokes (RANS) computations in combination with an FW-H acoustic analysis to study the aerodynamic and aeroacoustic performance of a series of NACA airfoils.

To enable a high-degree-of-freedom airfoil design or optimization, more efficient acoustic prediction schemes were

developed like the empirical method of Brooks, Pope, and Marcolini (BPM method) [5] which relates the noise emission to integral boundary-layer properties at the trailing edge. Parchen [6] proposed a more complex but nonetheless very efficient acoustic prediction method (TNO-TPD method) that takes the wall-normal distribution of relevant turbulence properties into account. This approach in combination with the XFOIL aerodynamic airfoil analysis code [7] was applied by Guidati and Wagner [8] to the first designs of low-noise airfoils for wind turbine applications. Later on, Moriarty et al. [9] modified the approach by calibrating some empirical constants in the model, based on comparisons of noise predictions to acoustic measurements.

The present trailing-edge noise prediction scheme also makes use of the TNO-TPD model but incorporates a more detailed calculation of the boundary-layer turbulence properties and a new semi-empirical scaling law for the vertical integral length scale which significantly increased the consistency of the airfoil noise prediction. The enhancements were developed in the European silent rotors by acoustic optimization project (SIROCCO) [10]. In this project, the noise reduction potential for modern wind turbines by designing and implementing new low-noise airfoils is being studied. The objective is to reduce the noise emission without loss in aerodynamic performance. At the beginning of the project, the consortium consisted of six participants, namely the Energy Research Centre of the Netherlands, the National Aerospace Laboratory (NLR) and Composite Technology Center (CTC) from The Netherlands, the University of Stuttgart and NOI Rotortechnik from Germany, and finally Gamesa Eólica from Spain. After the withdrawal of NOI and CTC, General Electric Wind Energy joined the project. In the frame of the project, new airfoils for the outer part of the blades had to be designed for three different reference turbines in the $1 \sim 2$ MW class. The airfoils were successfully wind-tunnel tested with respect to their aerodynamic and aeroacoustic characteristics. Currently, full-size blades are being manufactured to enable a final verification by field tests.

The present paper describes the prediction scheme used for the combined aerodynamic and aeroacoustic airfoil design along with recent enhancements of the model developed during the SIROCCO project. Detailed boundary-layer experiments and acoustic tests [11] were conducted in the laminar wind tunnel (LWT) of the Institute of Aerodynamics and Gas Dynamics (IAG) to improve and validate the prediction method. Representative results will be given. Finally, the airfoil design for the three reference turbines will be outlined and the results of the aerodynamic and acoustic wind-tunnel verification will be presented.

II. Prediction Model

A. Outline

Besides the computational aeroacoustics approach [12,13], several simplified but efficient schemes to predict the trailing-edge far-field noise have been developed [5,6,14–17]. Because the focus of the present investigation is on the design and high-degree-of-freedom numerical airfoil optimization, a highly efficient and robust prediction model was desired. Such an efficient method was developed by Parchen [6] at TNO-TPD on the basis of theories by Chandiramani [18], Blake [19], Chase [20], and Brooks and Hodgson [21]. Further on, this method shall be denoted as TNO-TPD model and will be discussed in more detail in Sec. II.C. With this approach, the unsteady surface pressure fluctuations, as induced by the convecting turbulent eddies, are described by a wave number frequency spectrum (k–ω spectrum), see Eq. (4) in Sec. II.C. The associated far-field noise emission is determined by evaluating the diffraction integral [Eq. (7) in Sec. II.C] for a semi-infinite flat plate [18]. The model gives the spectrum of the far-field noise for a specified observer distance without account for directivity. Parchen [6] developed a methodology to derive the k–ω spectrum from the boundary-layer mean profile in the vicinity of the trailing edge and the distribution of time-averaged turbulence data across the boundary layer. The required quantities (see Sec. II.C) except the vertical integral length scale (see Sec. II.D) can be calculated, for example, by means of an finite-difference boundary-layer code or a steady RANS analysis using a nonlinear nonalgebraic turbulence model or a Reynolds stress model.

B. Aerodynamic Model

In the course of an airfoil design process or a high-degree-of-freedom numerical optimization, RANS CFD calculations are usually much too time-consuming and the application of faster aerodynamic prediction methods as basis for the noise prediction is desired. In subsonic aerodynamic airfoil design, coupled panel boundary-layer methods, like Drela's XFOIL [7] are well established and have proven to provide a reliable prediction of the aerodynamic airfoil characteristics. The XFOIL code features an integral boundary-layer procedure that provides integral properties like displacement and momentum thickness or skin friction coefficient but no direct information about the wall-normal distribution of the mean velocity or turbulence properties.

To enable the coupling of the acoustic prediction model to airfoil analysis methods like XFOIL, Parchen developed an approach to derive the properties required to set up the k–ω spectrum from the output of integral boundary-layer procedures [6]. First of all, the unknown mean profile is approximated by a Coles law of the wall/law of the wake representation [22] showing the same boundary-layer thickness and skin friction as calculated by the boundary-layer procedure. From this approximated mean profile, the required turbulence properties are determined by means of a mixing-length approach and some semi-empirical relations [6].

Guidati and Wagner [8,23] used this approach to couple the TNO-TPD model to the XFOIL code to accomplish the design of low-noise laminar flow airfoils for wind turbine applications. The present author extended the method [24,25] by inclusion of the Swafford boundary-layer profile family [26], which also represents the basis for the turbulent closure relations in Drela's boundary-layer method [7].

This very efficient aerodynamic/aeroacoustic prediction method has turned out to yield quite reasonable results, at least for "usual" types of airfoil pressure distributions. However, one should be aware that the turbulence properties, which have a decisive impact on the predicted noise emission, are derived by means of a mixing-length approach based on the evaluation of the *local, approximated mean velocity profile*. The streamwise development of the turbulent fluctuations, its wall-normal distribution, and the growth of the turbulent eddies is not calculated directly, i.e., detailed history effects are not accounted for. History effects are only considered in a sense that its impact on the integral boundary-layer parameters is regarded by solving a lag-equation in Drela's method [7]. Moreover, the anisotropic behavior of the turbulent fluctuations is not modeled, but considered by a constant empirical anisotropy factor in the processing of the aerodynamic data. Because of these simplifications, it was expected that the scope of the determination of the turbulence properties and, finally, the noise prediction, is more or less limited to equilibrium boundary layers. Inaccuracies and inconsistencies in the predicted noise were expected to show up for types of pressure distributions with regions of strong flow deceleration or acceleration and also for cases with extended laminar flow and varying initial conditions for the turbulent region, e.g., downstream of a laminar separation bubble. Comparisons to detailed boundary-layer experiments confirmed this tendency [25].

Even small inconsistencies in the predicted noise spectra for different airfoil geometries, however, are problematic for the purpose of acoustic airfoil design because the impact of shape modifications on the noise emission has to be determined reliably, i.e., the method should give accurate results for relative differences in the noise spectra. The objective of the present investigations was, therefore, to improve the accuracy in the determination of the turbulence properties without losing the efficiency of the prediction scheme. To this end, the finite-difference (FD) boundary-layer code EDDYBL developed by Wilcox [22] was linked to the prediction model. With an FD method the boundary layer is discretized in streamwise and wall-normal direction and thus, the mean profile along with the

distribution of the time-averaged turbulence data is a direct result of the calculation. Among others, EDDYBL features a Reynolds stress turbulence model, namely the Wilcox stress-ω model, that accounts for anisotropy effects and provides the complete Reynolds stress tensor. Moreover, history effects are supposed to be captured more accurately compared with isotropic turbulence models [22].

To obtain the initial and boundary conditions for the EDDYBL analysis, a standard XFOIL analysis is performed in a first step. Because the governing equations for the outer flow and the boundary-layer analysis are solved simultaneously with XFOIL, the impact of the boundary-layer displacement effect is considered. The resulting outer flow velocity is then used as boundary condition for a subsequent EDDYBL analysis performed for the turbulent flow domain. The initial conditions are taken from the XFOIL boundary-layer analysis.

C. Noise Prediction Model

The present noise prediction scheme consists of two main steps. First, the spectrum of the surface pressure fluctuations at the trailing edge as induced by the turbulent eddies is described. In a second step, the noise emission from the trailing edge due to the fluctuating pressure is determined by solving the diffraction problem.

1. *Prediction of Surface Pressure Spectrum*

A turbulent boundary layer over a smooth, stationary, rigid surface at low Mach number is assumed. The equation for the pressure fluctuations in turbulence is derived by taking the divergence of the momentum equation, using the continuity equation to drop terms, performing a Reynolds decomposition into mean and unsteady terms, and then subtracting the time-averaged equation which finally yields

$$\nabla^2 p = -2\rho_0 \frac{\partial U_i}{\partial y_j}\frac{\partial u_j}{\partial y_i} - \frac{\partial^2}{\partial y_i \partial y_j}\rho_0(u_i u_j - \overline{u_i u_j}) \tag{1}$$

Equation (1) is a Poisson equation for the fluctuating pressure in a turbulent flow. The source terms on the right-hand side of Eq. (1) represent the mean shear-turbulence (MT) interaction (first term) and the turbulence-turbulence (TT) interaction (second term). Different authors (e.g., Lee et al. [27] or Blake [19]) showed that the contribution of the TT interaction is an order of magnitude smaller than the contribution of the MT interaction for wave numbers close to the convective wave number. The mean flowfield and turbulence describing these source terms can be obtained by solving the RANS equations together with an appropriate turbulence model. Equation (1) without TT source terms can be solved in the spectral domain. Adopting the standard boundary-layer approximations and the assumption that the flow in planes parallel to the wall is homogenous and stationary, Eq. (1) can be Fourier transformed in the two directions of these planes and over time. With these assumptions, the MT source term becomes $-2\rho_0[(\partial U_1/\partial y_2)(\partial u_2/\partial y_1)]$, where u_2 is the vertical fluctuation velocity. Following the derivations of Blake [19], a solution for the fluctuating pressure in a boundary layer above a rigid surface with MT as a source term can be obtained in terms of the spectral variable as

$$\hat{p}(\boldsymbol{k},\omega) = i\rho_0 \int_0^\infty \frac{\partial U_1}{\partial y_2}\frac{k_1 \hat{u}_2(y_2,\boldsymbol{k},\omega)}{\sqrt{k_0 - k^2}} e^{iy_2\sqrt{k_0-k^2}}\,\mathrm{d}y_2, \qquad k > k_0 \tag{2}$$

The wave number frequency spectrum of the wall pressure fluctuations that are homogenous in the 1, 3 plane is related to the modulus of $\hat{p}(\boldsymbol{k},\omega)$ according to

$$P(\boldsymbol{k},\omega)\delta(\boldsymbol{k}-\acute{\boldsymbol{k}})\delta(\omega-\acute{\omega}) = \langle p(\boldsymbol{k},\omega)p(\acute{\boldsymbol{k}},\acute{\omega})\rangle \tag{3}$$

where the angle brackets denote the ensemble average, $\boldsymbol{k} = [k_1, 0, k_3]$ is the wave number vector, and its magnitude in the 1, 3 plane is $|\boldsymbol{k}| = k = \sqrt{k_1^2 + k_3^2}$, $\hat{u}_2$ is the Fourier transform of the source density along the 1, 3 direction, and $k_0 = \omega|r|/c_0$.

Combining the preceding expression with Eq. (2), together with some assumptions $k \gg k_0, k_1 > \delta^{-1}$ and manipulations[6], yields an expression for the wave number frequency spectrum of the surface pressure fluctuations:

$$P(\boldsymbol{k},\omega) = 4\rho_0^2 \frac{k_1^2}{k_1^2 + k_3^2}\int_0^\infty \Lambda_2(y_2)\bar{u}_2^2\left(\frac{\partial U_1(y_2)}{\partial y_2}\right)^2 \Phi_{22}(\boldsymbol{k},\omega)\cdot\Phi_m[\omega - U_c(y_2)k_1]e^{-2|k|y_2}\,\mathrm{d}y_2 \tag{4}$$

In this equation, y_1 represents the streamwise, y_2 the wall-normal, and y_3 the spanwise direction. For the correlation function, the streamwise and spanwise directions are assumed to be homogenous in the boundary layer, i.e., the correlation function is the function of separation only in these directions. Here, $\bar{u}_2^2$ is the rms value of the vertical velocity fluctuations, U_1 is the streamwise mean velocity, U_c the convective velocity ($k_1 = \omega/U_c$), and Φ_{22} the spectrum of the vertical velocity fluctuations. The moving axis spectrum describes how the spectrum of the fluctuations is distorted by the generation and destruction of the eddies during their convection past the trailing edge. A Gaussian spectrum is used for Φ_m in the present method.

The Kármán three-dimensional kinetic energy density spectrum [19] $E(k)$ for isotropic turbulence represents the basis to derive the Φ_{22} spectrum:

$$E(k) = \frac{110\Gamma(5/6)}{27\sqrt{\pi}\Gamma(1/3)}\left(\frac{k_T}{k_e}\right)\frac{(k/k_e)^4}{[1+(k/k_e)^2]^{(17/6)}} \tag{5}$$

Again, assuming isotropic turbulence, the energy density spectrum for the vertical fluctuations in the k_1–k_3 plane reads as follows:

$$\Phi_{22}(k_1,k_3) = \frac{4}{9\pi}\cdot\frac{(k_1/k_e)^2 + (k_3/k_e)^2}{[1+(k_1/k_e)^2+(k_3/k_e)^2]^{7/3}}\cdot\bar{u}_2^2 \tag{6}$$

Thus, Eq. (4) represents a prediction model for the wave number frequency spectrum of the pressure fluctuations underneath a turbulent boundary layer as a function of time-averaged boundary-layer parameters (see Sec. II.B).

2. *Prediction of the Far-Field Noise*

Once the spectrum of the pressure fluctuations is known, the noise that is emitted from the trailing edge is calculated by representing the surface pressure fluctuations as a distribution of harmonic evanescent waves and solving the diffraction problem for these waves at the trailing edge according to Chandiramani [18]. The diffraction model for a semi-infinite plate is used, which, strictly speaking, limits the scope of the present approach to a frequency range where the airfoil can be considered as noncompact, i.e., the wavelength should be smaller than the chord length. Following Chase [20] and Brooks and Hodgson [21], the far-field pressure density can finally be expressed as

$$S(\omega) = \frac{L}{4\pi R^2}\int_{-\infty}^{\infty}\frac{\omega}{c_0 k_1}P(k_1,\omega)\,\mathrm{d}k_1 \tag{7}$$

D. Determination of the Vertical Integral Length Scale Λ_2

In the course of the present investigations, it turned out that the determination of the vertical integral length scale is the most crucial aspect in the processing of the turbulence data and that its accurate determination has a profound impact on the consistency of the noise prediction. Therefore, the present approach shall be discussed in more detail.

The length scale is related to the vertical extent of the turbulent eddies. More precisely, it is defined as the integral of the normalized spatial two-point correlation coefficient R_{22} of the vertical velocity fluctuations [19]:

$$\Lambda_2(y_2) = \int_0^\infty R_{22}\,\mathrm{d}r_2 = \int_0^\infty \frac{\overline{u_2(y_2,t)\cdot u_2(y_2+r_2,t)}}{\sqrt{\overline{u_2^2(y_2,t)}\cdot\overline{u_2^2(y_2+r_2,t)}}}\,\mathrm{d}r_2 \quad (8)$$

The length scale, however, is not provided by any established turbulence model or boundary-layer procedure. To derive Λ_2 from known quantities, usually, a calculated turbulence length scale or the mixing length is multiplied by an empirical scaling factor. As Λ_2 measurements are rarely published, a comparison of predicted and measured noise spectra may be used to derive the scaling factor.

For the present model, the derivation of an empirical scaling law based on a correlation of the predicted length scale to measured Λ_2 distributions was preferred. To establish a sound Λ_2 data base for subsonic airfoils, detailed boundary-layer experiments were performed in the laminar wind tunnel of the IAG. The suction side of three different airfoils was examined for clean (natural transition) and for tripped (forced transition at 5% chord) conditions at different angles of attack. Although one of these airfoils shows a small pressure rise in the turbulent region (light loading of the boundary layer), the others feature a quite strong main pressure recovery of different shape. Besides the mean velocity profile, the distributions of the velocity fluctuations and Λ_2 in the vicinity of the trailing edge were measured using miniature split-film probes [28].

When comparing the measured Λ_2 distributions to the length scale, as predicted by the present aerodynamic calculation method in combination with the stress-ω turbulence model (see Sec. II.B) it became obvious that a constant scaling factor is not sufficient to obtain good agreement for all test cases examined.

For this reason, another approach was followed relating Λ_2 to the wave number of the energy-bearing eddies rather than to use the length scale as a basis. For isotropic turbulence, Λ_2 is well defined in dependency of the wave number of the energy-bearing eddies [29]:

$$\Lambda_2 = \frac{\sqrt{\pi}\Gamma(5/6)}{\Gamma(1/3)}\cdot\frac{1}{k_e} \quad (9)$$

The wave number can be determined from the predicted turbulence kinetic energy and the dissipation rate following an approach by Lysak and Brungart [30]. The relation can be derived by comparing the asymptotic behavior of the Kármán spectrum (5) to the Kolmogorov spectrum for the inertial subrange:

$$E(k) = C\cdot\frac{\varepsilon^{2/3}}{k^{5/3}} \quad (10)$$

Here, C was found to be $C \approx 1.5$ according to experiments [30]. Equating the high wave number asymptote of Eqs. (5) and (10) yields

$$k_e = \left(\frac{1.5\cdot 27\sqrt{\pi}\Gamma(1/3)}{110\Gamma(5/6)}\right)^{3/2}\cdot\frac{\varepsilon}{(k_T)^{3/2}} \approx 1.9275\cdot\frac{\varepsilon}{(k_T)^{3/2}} \quad (11)$$

With Eq. (9), it finally follows

$$\Lambda_2 = \frac{\sqrt{\pi}\Gamma(5/6)}{\Gamma(1/3)}\cdot\frac{1}{\{[1.5\cdot 27\sqrt{\pi}\Gamma(1/3)]/[110\Gamma(5/6)]\}^{3/2}}\cdot\frac{(k_T)^{3/2}}{\varepsilon}$$
$$\approx 0.387\cdot\frac{(k_T)^{3/2}}{\varepsilon} \quad (12)$$

Because k_T and ε are provided by the stress-ω turbulence model used in the present prediction scheme, Eq. (12) allows one to determine Λ_2 on a sound basis. In fact, a better agreement to measured Λ_2 distributions could be achieved. Nonetheless, also for this approach, an additional scaling to match the experimental results turned out to be necessary. This may be attributed to the anisotropic behavior of the turbulence length scales. It was observed that, in general, for "heavily" loaded boundary layers (strong pressure rise), Λ_2 is underpredicted, whereas the tendency is reversed for a "lightly" loaded boundary layer. To consider this effect, an empirical scaling law was correlated to determine the final value of Λ_2 from the predicted value according to Eq. (12). A "loading parameter" was introduced representing the specific boundary-layer development.

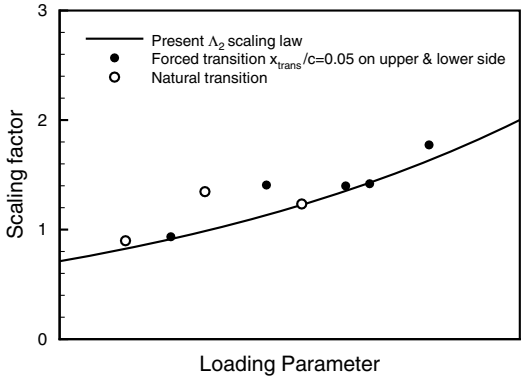

Fig. 1 Empirical Λ_2 scaling law.

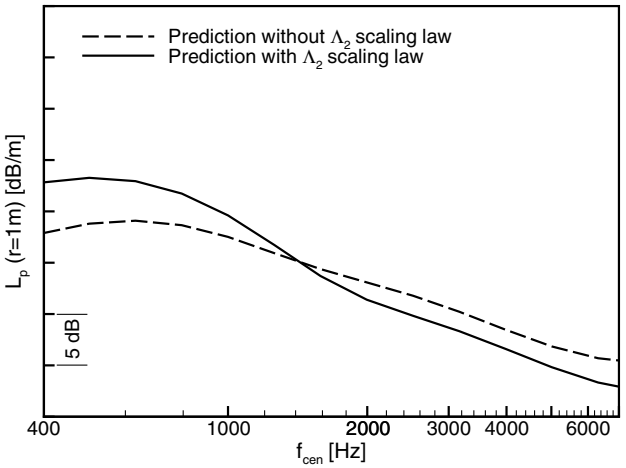

Fig. 2 Impact of the present Λ_2 scaling law on the predicted trailing-edge noise spectrum.

For each of the available test cases, the loading parameter was calculated and the scaling factor was determined from a comparison of the predicted Λ_2 distribution across the boundary layer to the measured one. The resulting correlation is depicted in Fig. 1.

To demonstrate the important impact of varying Λ_2 values on the noise level and to show the effect of the present Λ_2 scaling law, the predicted spectra for an exemplary airfoil analysis with and without application of the present scaling are given in Fig. 2. In this example, the scaling factor on the suction side is approximately 1.5, which is well within the range observed when comparing measured to calculated Λ_2 values (see Fig. 1).

III. Airfoil Design and Verification

In the course of the SIROCCO project, the blades of existing turbines should be modified by implementing new, silent airfoils in the outer part of the blades. Three reference turbines of different blade manufacturers were selected. To minimize the costs for the fabrication of the test blades, the use of existing molds or beams should be ensured as much as possible. This puts severe constraints on the geometric freedom of the airfoil design. Moreover, aerodynamic constraints, like a limitation of the acceptable shift of the lift curve, were to be considered. This limited the achievable noise reduction considerably.

The specific aerodynamic and aeroacoustic design objectives along with the constraints were defined in detail in a bilateral discussion with each industry partner. In general, the main objective was to minimize the A-weighted total sound pressure level for a given design lift region, while constraining the drag level to avoid a loss in performance compared with the airfoils used so far. In agreement with the general objective of the SIROCCO project, it was focused on a noise reduction for fully turbulent flow about the blades.

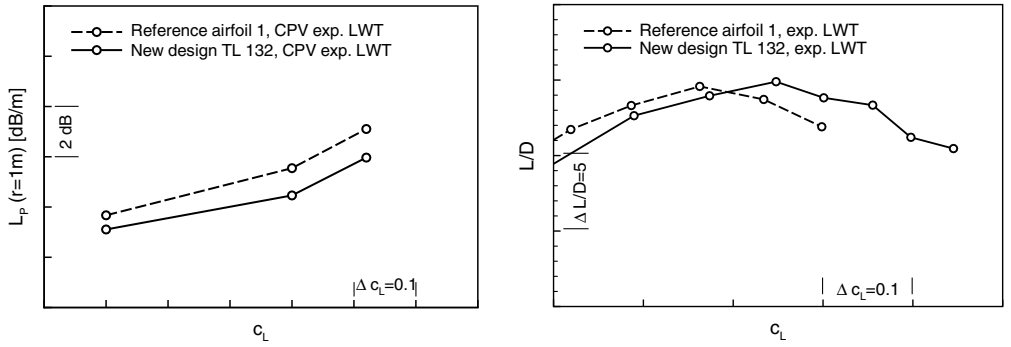

Fig. 3 Measured total sound pressure level and L/D of the first design, $Re = 1.6 \cdot 10^6$.

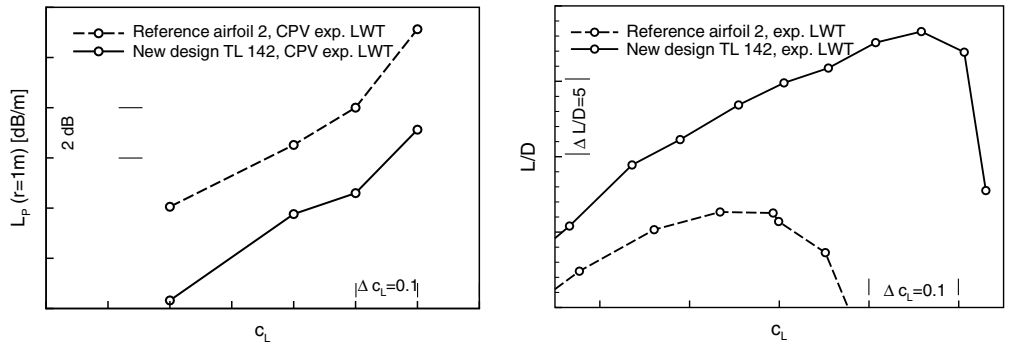

Fig. 4 Measured total sound pressure level and L/D of the second design, $Re = 1.6 \cdot 10^6$.

For fully turbulent flow and high lift coefficients, the value of L_p is clearly dominated by the noise contribution of the thick suction side boundary layer, which yields a peak in the spectrum in the low-frequency domain. For the considered applications, the peak frequency is typically in the range of 500 Hz $\sim$ 1 kHz and the corresponding wavelength is considerably smaller than the airfoil chord length ($\lambda_{\text{peak}} < c/2$), which justifies the application of the present diffraction model. To minimize L_p, the noise level has to be reduced, particularly around the peak frequency. This, in general, can be achieved by reducing the loading of the suction side boundary layer at the expense of an increased loading of the pressure side, which causes a slightly higher noise level at medium frequencies. Reducing the suction side loading, however, impacts the stall characteristics, which is a crucial issue for wind turbine airfoil design and needs special treatment.

As a first step in the airfoil design process, parametric investigations were performed to study the impact of certain geometric airfoil properties on the predicted noise emission. Thereafter, constrained direct numerical optimizations followed considering the aerodynamic and geometric constraints specified by the blade manufacturer. For this purpose, the present prediction model was coupled to the institute's optimization environment, Parallel Optimization Environment with modular structure (POEM) [25]. Basically, the optimizations were conducted because at the beginning of the project the acoustic airfoil design represented a quite new task and it was not clear a priori how all the constraints would impact the design. The optimizations were therefore intended to examine the constrained design space and to provide a good initial solution for the subsequent manual design, rather than to find the final airfoil shapes. In the authors' opinion, a manual "fine-tuning" of optimization results is important to consider the designer's experience in introducing qualitative design criteria, and in the interpretation and assessment of the prediction results. In particular, the prediction of the stall and poststall characteristics is a weak point with available analysis methods and requires an extensive experience-based interpretation.

In the subsequent manual design phase, the experience in acoustic airfoil design gathered in the frame of the SIROCCO project and the outcome of comparative acoustic airfoil measurements was considered along with the expertise in subsonic airfoil design at the IAG. The resulting airfoils for the three baseline turbines were wind-tunnel tested against their respective reference airfoils applied in the baseline blades so far. Results of polar measurements and acoustic tests performed in the LWT [11] are depicted in Figs. 3–5. The graphs show the characteristics around the respective main design point for tripped conditions applying turbulators on suction

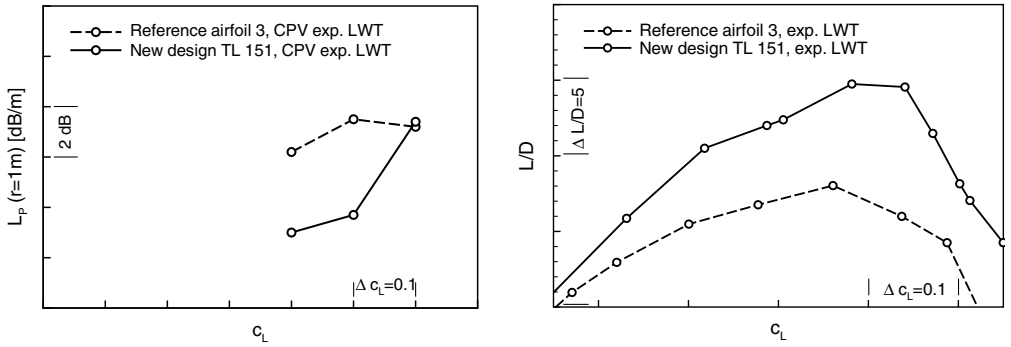

Fig. 5 Measured total sound pressure level and L/D of the third design, $Re = 3.0 \cdot 10^6$.

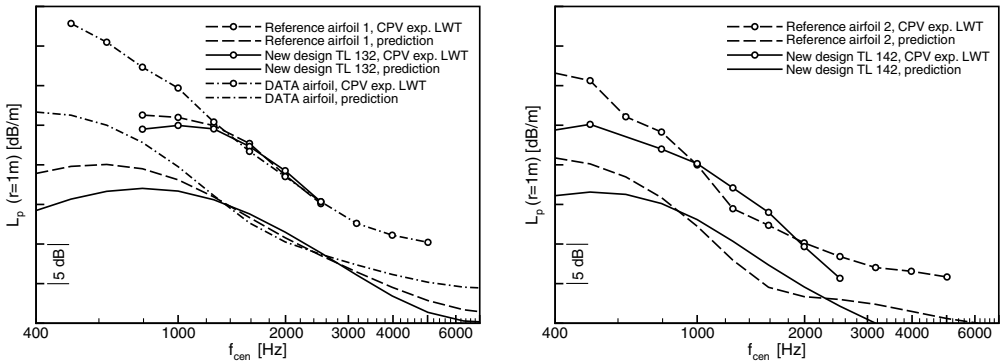

Fig. 6 Predicted and measured noise spectra of two new airfoils compared with their reference sections, $Re = 1.6 \cdot 10^6$, $c_L = 1.0$.

and pressure sides at 5% chord. Note that the axes are scaled differently in each figure. Therefore, no direct comparison between Figs. 3–5 is possible. For the first and the second airfoil (Figs. 3 and 4) the test Reynolds number was roughly half of the full-size conditions because a smaller chord length of the wind-tunnel models had to be chosen to enable parallel acoustic tests in the aeroacoustic wind tunnel Braunschweig (AWB).

In each figure, the left column gives the total sound pressure level vs c_L. The L_p values were obtained by an integration of the spectra as measured by means of the hot-wire based coherent particle velocity (CPV) technique [11,31]. The measurements show that a noise reduction compared with the reference sections could be achieved for all new airfoils. Thereby, the gain relates to the severity and number of constraints imposed in the airfoil design. Within the design region, the noise reduction ranges from about 1 dB up to 3.5 dB, see Figs. 3–5. It should be mentioned that the actual L_p reduction can be expected to be even slightly higher [25,32] because the new airfoils show a reduced noise level, especially in the low-frequency domain (see Fig. 6). Only the upper part of this low-frequency domain, however, can be measured accurately. In the L_p integration of the measured spectra, only the reliable frequency domain is considered, which means that the gain at very low frequencies is not reflected in the depicted L_p values. Two of the new airfoils tests were also conducted in the AWB applying a microphone array. This open-jet facility features an anechoic test chamber. The resulting total sound pressure level and the measured gain agrees quite well with the CPV results obtained in the LWT if appropriate open-jet wind-tunnel corrections for the lift coefficient and angle of attack are considered in the evaluation of the AWB results [11,32].

As can be seen from the right column in Figs. 3–5, the lift-to-drag ratio could also be increased or at least preserved with the new airfoils. Also, for the aerodynamic performance, the achieved gain directly relates to the severity of the imposed design constraints.

To demonstrate the accuracy of the present prediction method, a comparison of measured and predicted spectra for two of the new airfoils and their reference sections is given in Fig. 6. It should be mentioned that the shift in the absolute noise level between the experiments and the predictions stems from different distance scaling laws that were used to map the noise spectrum to a fictitious standard observer position. The related 7 dB difference in the noise level was not corrected to increase the clearness of the figures. It is obvious that the calculations quite accurately reproduce the shapes of the spectra and the relative differences between the airfoils. Noteworthy details like upper and lower crossing frequency and the overlapping of the compared spectra are exactly predicted. On the left-hand diagram, the spectrum of one airfoil examined in the previous European Design and Testing of Acoustically Optimized Airfoils with Wind Turbines (DATA) project is added. This airfoil was designed to feature reduced noise for *clean* conditions, not for tripped conditions as considered here.

Besides the examples shown, the complete calculation model was validated with respect to the prediction of relevant boundary-layer properties and the trailing-edge noise spectrum for various other airfoils at different freestream conditions. The comparisons to experiments performed in the LWT showed that the present model gives quite consistent results and correctly pictures the impact of different airfoil shapes or angle of attack. Compared with the previous approach based on an integral boundary-layer prediction, a noticeable improvement could be observed [25]. The extended method is nonetheless very efficient. One analysis for a single freestream condition typically requires on the order of 1 s CPU time on a PC.

IV. Conclusions and Outlook

An efficient scheme for the prediction of airfoil trailing-edge noise was implemented. Detailed boundary-layer experiments and measurements of the noise emission of subsonic airfoils, conducted in the laminar wind tunnel of the IAG, served to validate and to improve the theoretical model. The investigations have shown that the consideration of history and anisotropy effects during the calculation of the turbulence properties is important to establish a reliable and consistent noise prediction. The most crucial point in this respect was the correlation of an empirical scaling law to obtain the vertical integral length scale from turbulence data provided by the aerodynamic analysis. The consideration of these aspects improved the accuracy and consistency of the noise prediction significantly. This allowed use of the method for the purpose of acoustic airfoil design. Three different airfoils were developed for the outer blade region of three reference wind turbines. Wind-tunnel tests showed superior aeroacoustic behavior and also an improved aerodynamic performance compared with the reference sections used with the considered blades so far. This shows that a noise reduction without loss in performance is possible by a dedicated airfoil design. The total sound pressure level could be reduced by $1 \sim 3.5$ dB, even though severe geometric and aerodynamic constraints had to be considered in the design to enable the implementation to existing blade designs. The achieved gain directly relates to the severity of the imposed constraints. Currently, full-size blades featuring the new airfoils are being built and will be verified in field tests. For the acoustic tests, an array measurement technique (developed by NLR [33]) will be used, which enables researchers to localize and quantify noise sources on rotating blades.

Acknowledgments

Financial support for this research was given in part by the European Commission in the frame of the Fifth Framework Program. The authors would like to acknowledge the European Commission for supporting this research and the project partners for their good and fruitful cooperation.

References

[1] Oerlemans, S., and López, B. M., "Localisation and Quantification of Noise Sources on a Wind Turbine," *Wind Turbine Noise: Perspectives for Flow Control, Berlin, Germany, October 17–18, 2005* [CD-ROM], Institute of Noise Control Engineering, Meseyside, UK, 2005.

[2] Marsden, A. L., Wng, M., Dennis, J. E., Jr., and Moin, P., "Trailing-Edge Noise Reduction Using Derivative-Free Optimization and Large-Eddy Simulation," *Journal of Fluid Mechanics*, Vol. 572, 2007, pp. 13–

36.
[3] Ffowcs Williams, J. E., and Hall, L. H., "Aerodynamic Sound Generation by Turbulent Flow in the Vicinity of a Scattered Half Plane," *Journal of Fluid Mechanics*, Vol. 40, No. 4, 1970, pp. 657–670.
[4] Greschner, B., Yu, C., Zheng, S., Zhuang, M., Wang, Z. J., and Thiele, F., "Knowledge Based Airfoil Aerodynamic and Aeroacoustic Design," *11th AIAA/CEAS Aeroacoustics Conference, Monterey, CA*, AIAA Paper 2005-2968, 2005.
[5] Brooks, T. F., Pope, D. S., and Marcolini, M. A., "Airfoil Self-Noise and Prediction," NASA RP-1218, 1989.
[6] Parchen, R., "Progress Report DRAW: A Prediction Scheme for Trailing-Edge Noise Based on Detailed Boundary-Layer Characteristics," TNO Rept. HAG-RPT-980023, TNO Institute of Applied Physics, The Netherlands, 1998.
[7] Drela, M., "XFOIL: An Analysis and Design System for Low Reynolds Number Airfoils," *Low Reynolds Number Aerodynamics*, edited by T. J. Mueller, Univ. of Notre Dame Press, South Bend, IN, June 1989, pp. 1–12.
[8] Guidati, G., and Wagner, S., "Design of Reduced Noise Airfoils for Wind Turbines," *ECCOMAS 2000: European Congress on Computational Methods in Applied Sciences and Engineering*, European Community on Computational Methods in Applied Sciences, Barcelona, Spain, 2000.
[9] Moriarty, P. J., Guidati, G., and Migliore, P., "Prediction of Turbulent Inflow and Trailing-Edge Noise for Wind Turbines," *11th AIAA/CEAS Aeroacoustics Conference, Monterey, CA*, AIAA Paper 2005-2968, 2005.
[10] Schepers, J., Curvers, A., Oerlemans, S., Braun, K., Lutz, T., Herrig, A., Würz, W., and López, B. M., "SIROCCO: Silent Rotors by Acoustic Optimisation," *Wind Turbine Noise: Perspectives for Flow Control, Berlin, Germany, October 17–18, 2005* [CD-ROM], Institute of Noise Control Engineering, Meseyside, UK, 2005.
[11] Herrig, A., Würz, W., Lutz, T., and Krämer, E., "Trailing-Edge Noise Measurements Using a Hot-Wire Based Coherent Particle Velocity Method," *24th Applied Aerodynamics Conference, San Francisco, CA*, AIAA Paper 2006-3876, 2006.
[12] Ewert, R., and Schröder, W., "Simulation of Trailing Edge Noise with a Hybrid LES/APE Method," *Journal of Sound and Vibration*, Vol. 270, No. 3, 2004, pp. 509–524.
[13] Ewert, R., Meinke, M., and Schröder, W., "Computation of Trailing Edge Noise via LES and Acoustics Perturbation Equations," *8th AIAA/CEAS Aeroacoustics Conference and Exhibit, Breckenridge, CO*, AIAA Paper 2002-2467, 2002.
[14] Howe, M. S., "Review of the Theory of Trailing Edge Noise," *Journal of Sound and Vibration*, Vol. 61, No. 3, 1978, pp. 437–465.
[15] Grosveld, F. W., "Prediction of Broadband Noise from Horizontal Axis Wind Turbines," *Journal of Propulsion and Power*, Vol. 1, No. 4, July–Aug. 1985, pp. 292–299.
[16] Oberai, A., Roknaldin, F., and Hughes, T., "Computation of Trailing Edge Noise Due to Turbulent Flow over an Airfoil," *AIAA Journal*, Vol. 40, No. 11, 2002, pp. 2206–2216.
[17] Casper, J., and Farassat, F., "Trailing Edge Noise Prediction Based on a New Acoustic Formulation," AIAA Paper 2002-2447, 2002.
[18] Chandiramani, K., "Diffraction of Evanescent Wave with Application to Aerodynamically Scattered Sound and Radiation from Unbaffled Plates," *Journal of the Acoustical Society of America*, Vol. 55, No. 1, 1974, pp. 19–29.
[19] Blake, W., *Mechanics of Flow-Induced Sound and Vibration*, Vols. 1–2, Academic Press, New York, 1986.
[20] Chase, D. M., "Noise Radiated from an Edge in Turbulent Flow," *AIAA Journal*, Vol. 13, No. 8, Aug. 1975, pp. 1041–1047; also AIAA Paper 74-570, 1974.
[21] Brooks, T. F., and Hodgson, T. H., "Trailing Edge Noise Prediction from Measured Surface Pressures," *Journal of Sound and Vibration*, Vol. 78, No. 1, 1981, pp. 69–117.
[22] Wilcox, D. C., *Turbulence Modeling for CFD*, 2nd ed., DCW Industries, La Canada, CA, 1998, ISBN 0-9636051-5-1.
[23] Guidati, G., *Berechnung und Verminderung von Strömungsgeräuschen an Profilen*, Ph.D. Dissertation, Institute for Aerodynamics and Gas Dynamics, Univ. of Stuttgart, 2004.
[24] Lutz, T., Würz, W., Herrig, A., Braun, K., and Wagner, S., "Numerical Optimization of Silent Airfoil Sections," *DEWEK 2004: 7th German Wind Energy Conference, Wilhelmshaven, Germany, October 20/21, 2004* [CD-ROM], Deutsches Windenergie, Wilhelmshaven, Germany, 2004.
[25] Lutz, T., Herrig, A., Würz, W., Braun, K., and Krämer, E., "Constrained Aerodynamic & Aeroacoustic Design of Wind-Rotor Airfoils," *Wind Turbine Noise: Perspectives for Flow Control, Berlin, Germany, October 17–18, 2005* [CD-ROM], Institute of Noise Control Engineering, Meseyside, UK, 2005.
[26] Swafford, T. W., "Analytical Approximation of Two-Dimensional Separated Turbulent Boundary-Layer Velocity Profiles," *AIAA Journal*, Vol. 21, No. 6, 1983, pp. 923–925.
[27] Lee, Y. T., Blake, W., Farabee, T., Tse, M., and Brown, J., "Modelling of Wall Pressure Fluctuations Based on Time Mean Flowfield," *Journal of Fluids Engineering*, Vol. 127, No. 2, 2005, pp. 233–240.
[28] Herrig, A., and Würz, W., "Measurement of Transverse Correlation Lengths by Split-Film Probes," Univ. of Stuttgart, Internal Rept., Inst. of Aerodynamics and Gas Dynamics, July 2004.
[29] Mathieu, J., and Scott, J., *Introduction to Turbulent Flow*, Cambridge Univ. Press, Cambridge, England, U.K., 2000, ISBN 0-521-57066-2.
[30] Lysak, P., and Brungart, T., "Velocity Spectrum Model for Turbulence Ingestion Noise from Computational-Fluid-Dynamics Calculation," *AIAA Journal*, Vol. 41, No. 9, Sept. 2003, pp. 1827–1829.
[31] Würz, W., Guidati, S., Herrig, A., Lutz, T., and Wagner, S., "Measurement of Trailing Edge Noise by a Coherent Particle Velocity Method," *ICMAR 2004, Novosibirsk, 28 June–2 July, 2004*, Pt. 2, Inst. of Theoretical and Applied Science, Novosibirsk, Russia, 2004, pp. 195–200.
[32] Herrig, A., Würz, W., Lutz, T., Braun, K., Krämer, E., and Oerlemans, S., "Trailing-Edge Noise Measurements of Wind Turbine Airfoils in Open and Closed Test Section Wind Tunnels," *Wind Turbine Noise: Perspectives for Flow Control, Berlin, Germany, October 17–18, 2005* [CD-ROM], Institute of Noise Control Engineering, Meseyside, UK, 2005.
[33] Oerlemans, S., and López, B. M., "Acoustic Array Measurements on a Full Scale Wind Turbine," *11th AIAA/CEAS Aeroacoustics Conference, Monterey, CA*, AIAA Paper 2005-2963, 2005.

R. So
Associate Editor